2019 IMEKO TC-19 International Workshop on
Metrology for the Sea
Genoa, Italy, October 3-5, 2019

Shoreline measurement obtained with direct and remote techniques on a sandy beach in Gulf of Pozzuoli (Campania)

Giovanni Pugliano[1], Umberto Robustelli[1], Guido Benassai[1], Diana Di Luccio[2], Luigi Mucerino[3]

[1]*University of Naples "Parthenope", Engineering Department, Napoli, Italy*
[2]*University of Naples "Parthenope", Science and Technologies Department, Napoli, Italy*
[3]*University of Genova, Department of Earth, Environment and Life Sciences, Genova, Italy*

***Abstract* – In this paper the comparison between video-based and GPS-derived shoreline measurements was performed on a sandy beach located in the Gulf of Pozzuoli (Italy). The comparison between video camera and DGPS coastline has been carried out measuring the error as deviation from the DGPS line computed along the normal to DGPS itself. The deviations between the two dataset were examined in order to establish possible spatial dependence on video camera point of view in the intertidal zone. The results revealed that, generally, the error increases with the distance from the acquisition system. The comparison shows that the proposed model correctly represents the cameras error in coastline image extraction process.**

I. INTRODUCTION

Coastal areas are highly dynamic environments that provide important benefits but are also subject to a variety of natural hazards such as erosion, tsunamis and floods [1]. Understanding and predicting shoreline variability remains one of the main problems in coastal geomorphology and engineering. The dynamic nature of the shoreline and its dependence on the temporal and spatial scale at which it is being considered involves the use of a broad range of geomatic techniques. A number of data sources are available for shoreline positioning and mapping [2, 3], all presenting advantages and disadvantages. Direct shoreline surveys are normally carried out using GNSS technique by post-processing or real time methods [4]. The benefit of this technique is that it is higly accurate [5]; the main limitation is the huge time required for covering large stretches of the coastline and the difficulties inherent in doing ad-hoc timely post storm measurements. Shorelines may be derived by the application of digital image-processing techniques, airborne and satellite [6, 7] remote sensing provide the most common data sources for determinig shoreline positions. Land-based remote sensing technique is also available. Video monitoring can provide a remotely sensed measurement, fixed at a secure location (e.g. a tower or high-point), with the capability of acquiring imagery at a frequency ranging from fractions of seconds to hours. The technology is relatively low-cost, but the main issue is the processing method, especially the image rectification process, considering that the imagery is strongly oblique and relies on a number of GCPs (Ground Control Points) for finding the best geometry solutions. This technique has been successfully applied for both shoreline monitoring and rip current measurement [8, 9]. Based on this background, the research has focused on evaluate the potential errors resulting from the use of video monitoring system for the shoreline detection. The study area is a sandy beach located in the Gulf of Pozzuoli (Campania, Italy). The video shoreline remote observation was validated with the same measurements obtained during a Global Positioning System (DGPS) survey. The ability to detect the shoreline and its changes with video-monitoring techniques was checked to evidence possible errors and correlate them with the distance from viewpoint. The used statistical comparison model, suggested by Pugliano et al. [10], was tested in this new study area.

The paper is organized as follows: section ii. describes the used methods and data, section iii. presents the statistical results of the coastline data processing, section iv. draws the discussion of the obtained results, the conclusions and the future works.

II. METHODS AND DATA

A. *Beach video-monitoring*

In this study a video monitoring system was used to the shoreline detection along the beach (Fig. 1a). The video cameras was installed in proximity of a little beach (Fig. 2) in the Gulf of Pozzuoli (41°12'41.81"N;13°33'29.66"E). Two cameras (T1 and T2)) provide a total view of the beach with 1280x720 pixel resolution from an elevation of about 11 meters above Mean Sea Level (MSL). The images were collected every second from 8:00 until 16:00 local time and processed using Beachkeeper plus software [11] according to previous experience showed in Benassai et al. [12]. The video monitoring images were processed using time exposure images (or timex) methods; Shoreline detection from image is based on the physical consideration that the colour contrast between beach and water is

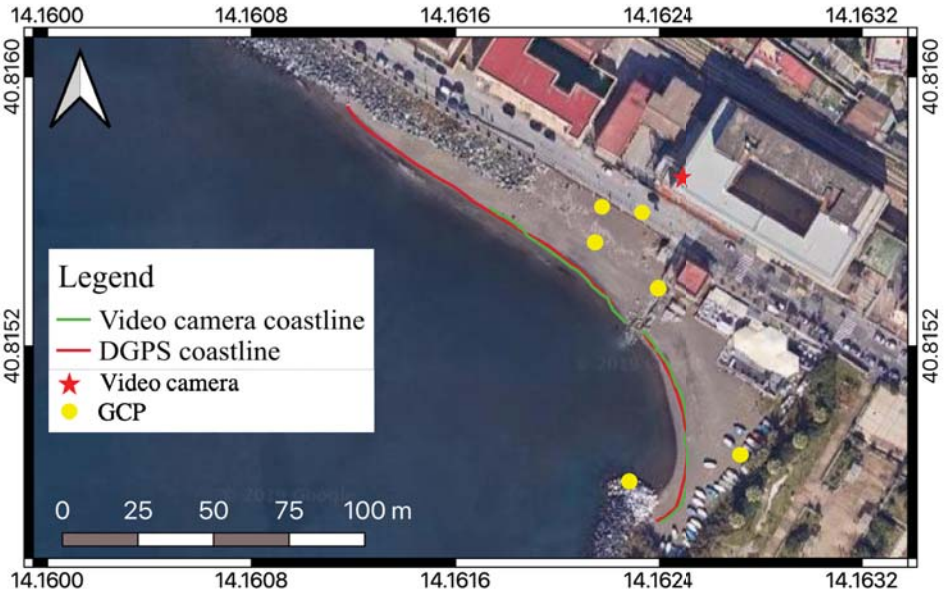

Fig. 1. Study area with video camera coastline (green line), DGPS coastline (red line), GCP (yellow circles) and video camera position (red star). (basemap ©2019 Google product).

sufficient, lighting is strong enough and the number of pixels in the water and beach groups is sufficient. Following [13] and other less recent Authors [14, 15, 16], the shoreline is detected using the swash signature on timex average images and its detection was based on the physical consideration that, when enlightenment and the picture are adequate, wet/dry boundary produces a visible color contrast easy to detect into the beach face. Finally, shorelines obtained from corresponding images from the two cameras are managed to form a whole continuous shoreline.

B. DGPS survey

DGPS survey was necessary to acquire the coastline position and to support the video-camera acquired dataset post-processing. In order to geo-rectify the video-derived images [17], a number of Ground Control Points (GCP), placed in the view area of cameras, were acquired in UTM-WGS84 using DGPS (Fig. 1a).

The surveying was employed also to get the reference shoreline position. The collection of shore-parallel GPS positions was carried out in 30th November 2018 using a single frequency, code and carrier phase receiver (Trimble Pathfinder ProXH) as rover.

C. Statistical comparison model

The comparison between video and DGPS coastline has been performed on the whole beach, measuring the error as deviation from the continuous DGPS line computed depicted in green along the normal to DGPS itself for a sample of about 200 points. These points were chosen keeping constant the mutual distance (about 0.6 m) along the track.

In this paper we tested the error model for video camera measurements developed by authors in Pugliano et al. [10] on the beach reported in Fig. 1a. The displacement offset with respect to the normal direction to the coastline ε_N (see Fig. 3) can be divided two components: ε_L representing the longitudinal error along the line of sight from the camera to the object and ε_T representing the transverse error, perpendicular to the line of sight. The angle α is the angle between the coastline and the line of sight. If α has been observed, then

$$\varepsilon_N = \varepsilon_L \sin\alpha + \varepsilon_T \cos\alpha \tag{1}$$

The longitudinal and transverse errors are computed from the following equation:

$$\varepsilon_L = \varepsilon_T = aD - be^{cs} \tag{2}$$

where D is the distance of the shoreline from the video camera, s is the intertidal beach slope, e is the Napier's constant, and a, b, c are three constants to be determined experimentally. In Equation 2 the correction be^{cs} may be applied to the distance-dependent error aD as the intertidal beach slope increases, which is in agreement with the inverse proportionality of the normal error with the beach slope [13].

Substituting Equation 2 into Equation 1, and if the longitudinal and transverse errors are grouped, yields

$$\varepsilon_N = (aD - be^{cs})(\sin\alpha + \cos\alpha) \tag{3}$$

Fig. 2. Video camera system installation point (red arrow) with its left (T1 camera) and right (T1 camera) points of view in (b) and (c), respectively..

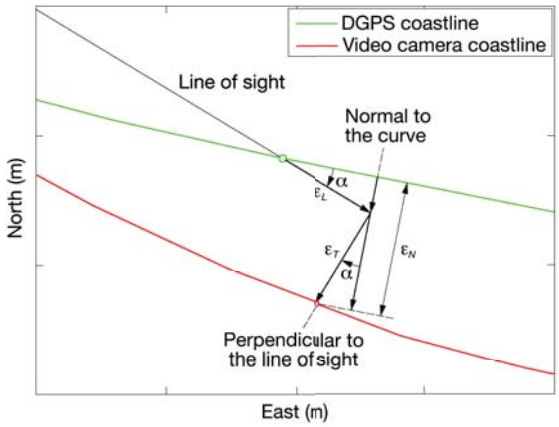

Fig. 3. Scheme of the longitudinal and transverse error projections along the normal direction to the coastline.

III. RESULTS

In Fig. 1 the video camera coastline (in green) and the DGPS one (in red) is reported for the whole beach.

In order to perform the error analysis it is useful to break the normal error into a distance-dependent part ε'_N and a slope-dependent one ε''_N.

The distance-dependent part can be estimated as:

$$\varepsilon'_N = aD\,(\sin\alpha + \cos\alpha) \tag{4}$$

where the constant a is computed experimentally from the field data; the values were 0.015 and 0.01 for the North side camera (from 0–32 m) and the South side camera (from 32–134 m), respectively.

In performing normal error estimation, it is assumed that there are possible corrections due to the increasing intertidal beach slope. The model adopted to estimate these corrections is:

$$\varepsilon''_N = be^{cs}\,(\sin\alpha + \cos\alpha) \tag{5}$$

Nevertheless, in this work we do not consider the slope so the error is fully represented by Equation 4.

Substituting the appropriate values into Equation (4), yields:

$$\varepsilon'_N = 0.015D\,(\sin\alpha + \cos\alpha) \tag{6}$$

for north camera and

$$\varepsilon'_N = 0.01D\,(\sin\alpha + \cos\alpha) \tag{7}$$

for south camera.

The result depends on the combination of two components including camera distance D and the angle α between the coastline and the line of sight. The error model for video camera measurements was tested for the entire study area. Figure 4 shows the estimated normal errors determined by the final computed Equation (4). The positive (negative) values indicate seaward (landward) offsets of the shoreline. The red curve represents normal errors that increase with the distance compared to the observed values (light blue curve).

The observation of Fig. 4 suggests that the particular combination produced results corresponding to those observed for the whole beach. In particular, for the northern camera image the error was around $\pm$ 1 m, while for the south camera images a discontinuity with a maximum value of 1 m happens near 105 m.

IV. DISCUSSION AND CONCLUSIONS

In this paper, a shoreline detection technique from a low-cost video monitoring station was used, applying an automatic extraction technique that undertakes a water/beach

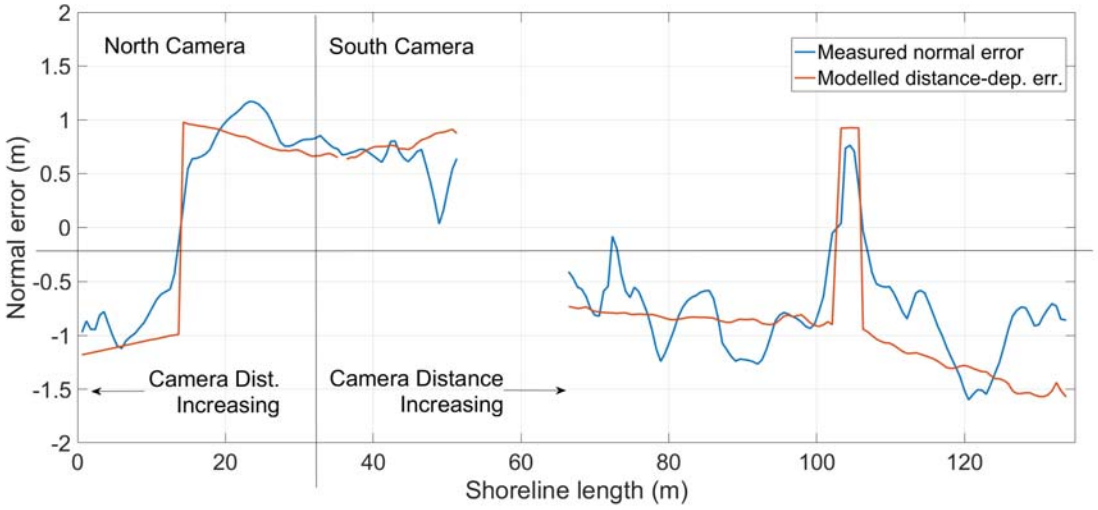

Fig. 4. Estimated normal error.

distinction from color band ratios and a shoreline slope recognition module.

Compared to a direct DGPS survey, the video-derived coastline acquisition was less time consuming and more cost effective. The possibility to acquire a beach topography with a high temporal frequency can potentially highlight coastal processes during the winter season, when a direct survey is difficult due to harsh weather conditions. The error model, based on the transverse and longitudinal error along the line of sight used gives good results.

Day-light limitations of the video-derived data can be overcome by thermal cameras, which can operate also during night hours in order to monitor the beach during severe events. This goal will be the continuation of the present research, together with the challenge of modeling new algorithms to lower the deviation from direct measurements. Some related avenues of research that should be pursued include further validation comparing the coastline obtained with the cameras and that obtained with a dual frequency GPS survey. In fact, as amply demonstrated in [18, 19, 20, 21, 22, 23, 24, 25, 26, 27, 28] single frequency receivers are affected by errors that can be mitigated with by using double frequency receivers.

V. ACKNOWLEDGMENTS

This research is partially included in the framework of the project ABBACO. The authors are grateful to I.P.S.E.O.A "Rossini" for hosting the video camera system and to the forecast service of the University of Napoli "*Parthenope*" (`http://meteo.uniparthenope.it`) for the HPC facilities.

REFERENCES

[1] F. Nunziata, A. Buono, M. Migliaccio, and G. Benassai, "Dual-polarimetric c-and x-band sar data for coastline extraction," IEEE Journal of Selected Topics in Applied Earth Observations and Remote Sensing, vol. 9, no. 11, pp. 4921–4928, 2016.

[2] E. Boak and I. Turner, "Shoreline definition and detection: A review," Journal of Coastal Research, vol. 21, no. 4, pp. 688–703, 2005.

[3] D. Dominici, K. LELO, V. BAIOCCHI, and P. Francesco, "Geomatic methodologies for the extraction of coastal areas," in Il Monitoraggio Costiero Mediterraneo: problematiche e, vol. 1, pp. 20–28, 2010.

[4] R. A. Morton, M. P. Leach, J. G. Paine, and M. A. Cardoza, "Monitoring beach changes using gps surveying techniques," Journal of Coastal Research, pp. 702–720, 1993.

[5] M. J. Pajak and S. Leatherman, "The high water line as shoreline indicator," Journal of Coastal Research, pp. 329–337, 2002.

[6] R. Holman and M. C. Haller, "Remote sensing of the nearshore," Annual Review of Marine Science, vol. 5, pp. 95–113, 2013.

[7] F. Palazzo, D. Latini, V. Baiocchi, F. Del Frate, F. Giannone, D. Dominici, and S. Remondiere, "An application of cosmo-sky med to coastal erosion studies," European Journal of Remote Sensing, vol. 45, no. 1, pp. 361–370, 2012.

[8] K. T. Holland, R. A. Holman, T. C. Lippmann, J. Stanley, and N. Plant, "Practical use of video imagery in nearshore oceanographic field studies," IEEE Journal of oceanic engineering, vol. 22, no. 1, pp. 81–92, 1997.

[9] S. G. J. Aarninkhof, "Nearshore bathymetry derived from video imagery," 2003.

[10] G. Pugliano, U. Robustelli, D. Di Luccio, L. Mucerino, G. Benassai, and R. Montella, "Statistical deviations in shoreline detection obtained with direct and remote observations," Journal of Marine Science and Engineering, vol. 7, no. 5, 2019.

[11] M. Brignone, C. F. Schiaffino, F. I. Isla, and M. Ferrari, "A system for beach video-monitoring: Beachkeeper plus," Computers & geosciences, vol. 49, pp. 53–61, 2012.

[12] G. Benassai, D. Di Luccio, L. Mucerino, G. D. Paola, C. M. Rosskopf, G. Pugliano, U. Robustelli, and R. Montella, "Shoreline rotation analysis of embayed beaches in the central thyrrenian sea," in 2018 IEEE International Workshop on Metrology for the Sea; Learning to Measure Sea Health Parameters (MetroSea), pp. 7–12, Oct 2018.

[13] R. Almar, R. Ranasinghe, N. Sénéchal, P. Bonneton, D. Roelvink, K. R. Bryan, V. Marieu, and J.-P. Parisot, "Video-based detection of shorelines at complex meso–macro tidal beaches," Journal of Coastal Research, vol. 28, no. 5, pp. 1040–1048, 2012.

[14] S. Aarninkhof, "Argus-based monitoring of intertidal beach morphodynamics," in Proceedings of Coastal Sediments 99, 1999.

[15] P. S. Alexander and R. A. Holman, "Quantification of nearshore morphology based on video imaging," Marine geology, vol. 208, no. 1, pp. 101–111, 2004.

[16] M. Davidson, S. Aarninkhof, M. Van Koningsveld, and R. Holman, "Developing coastal video monitoring systems in support of coastal zone management," Journal of Coastal research, pp. 49–56, 2006.

[17] L. Mucerino, M. Albarella, L. Carpi, G. Besio, A. Benedetti, N. Corradi, M. Firpo, and M. Ferrari, "Coastal exposure assessment on bonassola bay," Ocean & coastal management, vol. 167, pp. 20–31, 2019.

[18] U. Robustelli and G. Pugliano, "Assessment of pseudorange measurements of galileo foc satellites with incorrect highly eccentric orbits," vol. 2116, 2019.

[19] U. Robustelli and G. Pugliano, "Galileo single point positioning assessment including foc satellites in eccentric orbits," Remote Sensing, vol. 11, no. 13, 2019.

[20] U. Robustelli, G. Benassai, and G. Pugliano, "Signal in space error and ephemeris validity time evaluation of milena and doresa galileo satellites," Sensors (Switzerland), vol. 19, no. 8, 2019.

[21] U. Robustelli and G. Pugliano, "Code multipath analysis of galileo foc satellites by time-frequency representation," Applied Geomatics, vol. 11, no. 1, pp. 69–80, 2019.

[22] U. Robustelli, G. Benassai, and G. Pugliano, "Accuracy evaluation of doresa and milena galileo satellites broadcast ephemerides," pp. 217–221, 2019.

[23] U. Robustelli, V. Baiocchi, and G. Pugliano, "Assessment of dual frequency gnss observations from a xiaomi mi 8 android smartphone and positioning performance analysis," Electronics (Switzerland), vol. 8, no. 1, 2019.

[24] U. Robustelli and G. Pugliano, "Gnss code multipath short-time fourier transform analysis," Navigation, Journal of the Institute of Navigation, vol. 65, no. 3, pp. 353–362, 2018.

[25] G. Pugliano, U. Robustelli, F. Rossi, and R. Santamaria, "A new method for specular and diffuse pseudorange multipath error extraction using wavelet analysis," GPS Solutions, vol. 20, no. 3, pp. 499–508, 2016.

[26] A. Angrisano, S. Gaglione, C. Gioia, M. Massaro, and U. Robustelli, "Assessment of nequick ionospheric model for galileo single-frequency users," Acta Geophysica, vol. 61, no. 6, pp. 1457–1476, 2013.

[27] A. Angrisano, S. Gaglione, C. Gioia, U. Robustelli, and M. Vultaggio, "Giove satellites pseudorange error assessment," Journal of Navigation, vol. 65, no. 1, pp. 29–40, 2012.

[28] S. Gaglione, A. Angrisano, G. Pugliano, U. Robustelli, R. Santamaria, and M. Vultaggio, "A stochastic sigma model for glonass satellite pseudorange," Applied Geomatics, vol. 3, no. 1, pp. 49–57, 2011.